Verotoxin and ricin have novel effects on preproendothelin-1 expression but fail to modify nitric oxide synthase (ecNOS) expression and NO production in vascular endothelium.

M M Bitzan, … , J Lin, P A Marsden

J Clin Invest. 1998;101(2):372-382. https://doi.org/10.1172/JCI522.

Research Article

Interaction of bipartite Escherichia coli O157-derived verotoxins (VTs) 1 and 2 (Shiga toxin 1 and 2) with vascular endothelium is believed to play a central role in the pathogenesis of the thrombotic microangiopathy and ischemic lesions characteristic of hemolytic uremic syndrome and of E. coli O157-associated hemorrhagic colitis. We defined the effects of VTs on the expression of potent endothelial cell-derived regulators of vascular wall function, namely endothelin-1 (ET-1) and nitric oxide (NO). In quiescent bovine aortic endothelial cells, both VT1 and VT2, but not receptor-binding VT B-subunit which lacks N-glycosidase activity, induced concentration-dependent (0.1-10 nM) increases in steady state preproET-1 mRNA transcript levels, an effect that was maximal at 12-24 h. Metabolic-labeling experiments indicated that VTs increased preproET-1 mRNA transcript levels at concentrations that had trivial effects on nascent DNA, RNA, and protein synthesis. In contrast to preproET-1, endothelin converting enzyme-1 and endothelial constitutive NO synthase mRNA transcript levels remained unchanged. Consistent with these findings, VTs failed to modulate immunoreactive endothelial constitutive NO synthase expression and basal and calcium-dependent L-[14C]arginine to L-[14C]citrulline conversion or the NO chemiluminescence signal. The plant-derived toxin ricin, which shows a similar molecular mechanism of enzymatic ribosomal modification to VTs, caused comparable effects on these endothelial vasomediators and metabolite incorporation, at 3 log orders lower concentrations. Nuclear transcription and actinomycin D chase experiments indicated that […]

Verotoxin and Ricin Have Novel Effects on Preproendothelin-1 Expression but Fail to Modify Nitric Oxide Synthase (ecNOS) Expression and NO Production in Vascular Endothelium

Martin M. Bitzan, Yang Wang, Janie Lin, and Philip A. Marsden
Division of Nephrology, Department of Medicine, St. Michael's Hospital and University of Toronto, Toronto, Ontario, Canada M5S 1A8

Abstract

Interaction of bipartite *Escherichia coli* O157-derived verotoxins (VTs) 1 and 2 (Shiga toxin 1 and 2) with vascular endothelium is believed to play a central role in the pathogenesis of the thrombotic microangiopathy and ischemic lesions characteristic of hemolytic uremic syndrome and of *E. coli* O157-associated hemorrhagic colitis. We defined the effects of VTs on the expression of potent endothelial cell–derived regulators of vascular wall function, namely endothelin-1 (ET-1) and nitric oxide (NO). In quiescent bovine aortic endothelial cells, both VT1 and VT2, but not receptor-binding VT B-subunit which lacks *N*-glycosidase activity, induced concentration-dependent (0.1–10 nM) increases in steady state preproET-1 mRNA transcript levels, an effect that was maximal at 12–24 h. Metabolic-labeling experiments indicated that VTs increased preproET-1 mRNA transcript levels at concentrations that had trivial effects on nascent DNA, RNA, and protein synthesis. In contrast to preproET-1, endothelin converting enzyme-1 and endothelial constitutive NO synthase mRNA transcript levels remained unchanged. Consistent with these findings, VTs failed to modulate immunoreactive endothelial constitutive NO synthase expression and basal and calcium-dependent L-[^{14}C]arginine to L-[^{14}C]citrulline conversion or the NO chemiluminescence signal. The plant-derived toxin ricin, which shows a similar molecular mechanism of enzymatic ribosomal modification to VTs, caused comparable effects on these endothelial vasomediators and metabolite incorporation, at 3 log orders lower concentrations. Nuclear transcription and actinomycin D chase experiments indicated that VTs stabilize labile preproET-1 mRNA transcripts in endothelial cells. Therefore, VTs potently increase select mRNA transcript levels in endothelial cells at concentrations of toxins that have minimal effects on protein synthesis. Perturbed expression of endothelial-derived vasomediators may play a pathophysiologic role in the microvascular dysfunction that is the hallmark of hemolytic uremic syndrome and hemorrhagic colitis. (*J. Clin. Invest.* 1998. 101: 372–382.) **Key words: hemolytic uremic syndrome • endothelin-1 • nitric oxide synthase • mRNA • endothelin-converting enzyme-1**

Introduction

Verotoxins (VTs)[1] (Shiga toxins) comprise a family of structurally related, bipartite protein exotoxins produced by *Escherichia coli*, especially serotype O157:H7 (1). VT1 and VT2 have been implicated by epidemiologic, microbiologic, and cellular biology studies in the pathogenesis of hemorrhagic colitis and hemolytic uremic syndrome (HUS) in humans (2–4). VT2e has been identified as the cause of systemic edema disease of weaning piglets (5). Characteristic histopathologic and pathophysiologic features of VT-associated HUS include thrombotic microangiopathy, focal areas of ischemia, and, in some settings, profound hypertension (6–9). Though there is abundant evidence of platelet–microvascular endothelial interaction, perturbation of the fibrinolytic cascade, and arachidonic acid metabolism (7, 10, 11), the precise disease mechanisms remain enigmatic (4, 12).

VTs bind with high affinity to the membrane-anchored glycosphingolipids globotriosylceramide (Gb3) and globotetraosylceramide (Gb4). Glycolipid binding is mediated by the lectin-like, pentameric B subunit of VTs (13). Retrograde intracellular transport of endocytosed VT to the endoplasmic reticulum via the Golgi apparatus (14) is a prerequisite for the protein-synthesis–inhibiting action of the toxins (1). The VT A subunit displays structural and functional homology with the A subunit of ricin, a heterodimeric lectin derived from the seeds of the castor oil plant (*Ricinus communis*) (15, 16). The 32-kD ricin A chain is linked by a disulfide bond to a single B chain of similar size which mediates membrane receptor binding and internalization (14, 15). This contrasts with the noncovalent, 1:5 stoichiometric relationship of the A:B subunits in VTs (1). The A subunits of VT and ricin possess intrinsic *N*-glycosidase activity. In cell-free systems they both hydrolyze a specific adenine residue at position 4324 of the 28S ribosomal RNA of the 60S mammalian ribosomal subunit. This posttranscriptional modification leaves the phosphodiester bond intact, but effectively interferes with the binding and coordinated function of eukaryotic elongation factors EF-1 and -2 (1, 16, 17).

We hypothesized that endothelial cell activation plays an important role in the pathophysiology of VT-associated disease, specifically HUS. A paucity of data is available on the endothelial genes implicated in the pathobiology of endothe-

Address correspondence to Dr. Philip A. Marsden, University of Toronto, Medical Sciences Bldg., Rm. 7358, 1 King's College Circle, Toronto, ON, Canada M5S 1A8. Phone: 416-978-2441; FAX: 416-978-8765; E-mail: p.marsden@utoronto.ca

Received for publication 5 May 1997 and accepted in revised form 14 November 1997.

J. Clin. Invest.

0021-9738/98/01/0372/11 $2.00
Volume 101, Number 2, January 1998, 372–382
http://www.jci.org

1. *Abbreviations used in this paper:* BAEC, bovine aortic endothelial cell; ECE, endothelin converting enzyme; ecNOS, endothelial constitutive nitric oxide synthase; ET-1, endothelin-1; GAPDH, glyceraldehyde-3-phosphate dehydrogenase; Gb3, globotriosylceramide; Gb4, globotetraosylceramide; HUS, hemolytic uremic syndrome; UTR, untranslated region; VT, verotoxin.

lial dysfunction in VT-associated HUS. Endothelial-derived nitric oxide (NO) radical and the peptide endothelin-1 (ET-1) are major paracrine and autocrine mediators which, among others, regulate local blood flow and, in the case of NO, modulate platelet adhesion, aggregation, and degranulation (18, 19). We speculated that VT might perturb the expression of these vasomediators in vascular endothelium. Therefore, the purpose of this study was to define the effects of VTs and of ricin on the expression of these endothelial-derived vasomediators using a well characterized, robust endothelial culture model (20).

Methods

Materials. Cell culture reagents, dithiothreitol, and MMLV reverse transcriptase polymerases were from GIBCO BRL (Grand Island, NY). Bovine calf serum (low endotoxin) was purchased from Hyclone Laboratories (Logan, UT). Cell culture plates were from Corning Inc. (Corning, NY). Ionomycin was from Calbiochem (La Jolla, CA). Deoxynucleotidetriphosphates were from Boehringer Mannheim GmbH (Mannheim, Germany), restriction enzymes from New England Biolabs (Beverly, MA), RNases A and T from Ambion (Austin, TX), and DNase 1 and RNase inhibitor from Promega (Madison, WI). Guanidinium thiocyanate was from Fluka Biochemika (Buchs, Switzerland). L-[^{14}C]arginine (sp act 300 Ci/mmol), Hybond^{+} nylon membranes, ET-1 radioimmunoassay kit (21 peptide-specific), and enhanced chemiluminescence substrate were from Amersham (Arlington Heights, IL). SepPak C18 cartridges were from Waters Millipore Corp. (Milford, MA). Protran nitrocellulose membranes were from Schleicher and Schuell (Keene, NH). Bradford method–based protein assay (protein assay kit II) and Dowex AG 50WX-8 cation exchange resin (Na^{+} form, 100–200 mesh) were from Bio-Rad (Hercules, CA). Deoxycytidine 5′-[α-^{32}P]triphosphate ([α-^{32}P]dCTP; 3,000 Ci/mmol), uridine 5′-[α-^{32}P]triphosphate ([α-^{32}P]UTP; 3,000 Ci/mmol), L-[3,4,5-^{3}H(*N*)]leucine ([^{3}H]leucine; > 140 Ci/mmol), [methyl-^{3}H]thymidine ([^{3}H]thymidine; 70–90 Ci/mmol), [5,6-^{3}H]uridine ([^{3}H]uridine; 35–50 Ci/mmol) were purchased from DuPont-NEN (Boston, MA). Mouse monoclonal IgG against human endothelial constitutive nitric oxide synthase (ecNOS) protein was from Transduction Laboratories (Lexington, KY). Horseradish-conjugated sheep anti–mouse IgG antibody was from Bio-Rad. Other reagents were from Sigma Chemical Co. (St. Louis, MO). VTs were purified to homogeneity from defined *E. coli* strains by sequential chromatography in the laboratories of Drs. M.A. Karmali (The Hospital for Sick Children, Toronto, Canada) and J.L. Brunton (The Toronto Hospital, Toronto, Canada) (0.6–3.1 mg protein/ml, cytotoxic titers [Vero cells] $\sim 10^{-8}$ for the holotoxins, $< 10^{-2}$ for the pentameric VT1 B subunit) as described previously (21–23). VT preparations contained negligible amounts of endotoxin (at or less than the detection limit of 0.05 endotoxin units/ml) (E-toxic assay; Sigma Chemical Co.) (24). Highly purified ricin was purchased from Sigma Chemical Co. (RCA_{60}). Toxin aliquots were stored at −80°C and diluted in serum-free medium immediately before experimentation.

Cell culture. Bovine endothelial cells were isolated from the thoracic aorta of calves and phenotypically characterized as described previously (25). Single-clone, homogeneous bovine aortic endothelial cell (BAEC) cultures were serially passaged on 0.2% gelatin-coated 100-mm dishes after digestion with trypsin-EDTA (0.05%) and propagated in RPMI 1640 medium containing 15% bovine calf serum, penicillin G (100 U/ml), and streptomycin sulfate (100 μg/ml). For the majority of experiments, cells were used at passages 4 and 5. To examine the effect of VT on BAEC, 100-mm dishes were plated at a density of 5–10 × 10^{5} cells per dish in 10 ml complete medium. 2 d after reaching confluence, generally 5 d after splitting, complete medium was replaced by serum-free medium, and cells were harvested 48 h later. Toxin was added at the indicated concentrations 24 h before harvesting, unless stated otherwise.

Metabolite pulse labeling. Cells were grown 2 d after confluence in 24-well dishes containing 0.4 ml complete RPMI medium. The medium was changed to serum-free RPMI 24 h before toxin or vehicle was added. 1 h before harvest, 1 μCi of [^{3}H]thymidine, [^{3}H]uridine, or [^{3}H]leucine was added per well. Monolayers were rapidly washed with ice-cold PBS to terminate isotope uptake, incubated with 0.5 ml of 15% TCA at 4°C for 20 min, and rinsed twice with ice-cold H_2O. Cell-associated radioactivity was determined after solubilization with 0.1 M NaOH-0.1% SDS (wt/vol). Aliquots from each well were removed for scintillation counting. Data were normalized against vehicle-treated controls with no added toxin. Results of three independent experiments, each performed in triplicate, were expressed as arithmetic means±SEM.

Molecular cloning and cDNA probes. Random-primed, first strand complementary DNA (cDNA) was prepared from total cellular RNA isolated from BAEC using MMLV reverse transcriptase (26). A 744-bp DNA fragment for coding sequences of bovine endothelin converting enzyme-1 (ECE-1) was generated by PCR (sense primer BE-1: 5′ GCT CCT GGC GGC GGC ATT GGT G 3′; antisense primer BE-2: 5′ TCC TGG GGG ATG GTG ATG TTG G 3′), cloned into the pCRII vector and subjected to dideoxynucleotide sequence analysis. A BstXI restriction enzyme fragment of the cloned bovine ECE-1 cDNA corresponding to amino acids 58–305 was used as a probe. The 1.4-kb EcoRI restriction enzyme fragment of pBov ET-1 containing the open reading frame of bovine preproET-1 was described previously (27). A 5′-preproET-1 cDNA probe containing the first 360 bp (exons 1–3), and a 1 kb 3′-preproET-1 probe containing the remaining sequences (exons 4–5) were obtained by digestion of pBovET-1 with NcoI and EcoRI. The 1.9-kb EcoRI restriction enzyme bovine ecNOS cDNA clone pBov3′NOS corresponding to exons 15–26 of the human ecNOS gene has been described (28). A 551-bp 5′ bovine ecNOS cDNA fragment corresponding to exons 1–4 of human ecNOS was generated by EcoRI/SfiI digestion of the 1785-bp EcoRI restriction enzyme clone pBov5′NOS (28). A HindIII/XbaI restriction fragment of GAPDH (20) encompassing 547 bp of the human glyceraldehyde-3-phosphate dehydrogenase cDNA and a 0.75-kb BamH1/Sph1 restriction fragment of 18S ribosomal RNA cDNA (29) were used for normalization in Northern and actinomycin D chase experiments, respectively.

Northern blot analysis. Total cellular RNA was extracted using the guanidinothiocyanate-phenol-chloroform procedure, size-fractionated by electrophoresis through denaturing (1% agarose-0.66 M formaldehyde) gels, transferred onto nylon membranes, UV cross-linked, and hybridized using published methods (30). Gels were stained with ethidium bromide to verify loading of comparable amounts of intact RNA. Membranes were prehybridized at 42°C in 50% deionized formamide, 6× SSPE, 5× Denhardt's solution, 0.5% SDS, and 100 μg/ml denatured salmon sperm DNA (hybridization solution), for a minimum of 4 h. Gel-purified cDNA probes were labeled to a sp act of ≥ 10^{9} cpm/μg with [α-^{32}P]dCTP by the random primer labeling method. Hybridization was carried out with 10^{6} cpm/ml in fresh hybridization solution at 42°C for 18–24 h. Membranes were washed under high stringency conditions and monitored with a Geiger counter. Radioactive signals were recorded using a PhosphorImager (Molecular Dynamics, Sunnyvale, CA) and quantitated using ImageQuant software 4.2 for Windows NT (Molecular Dynamics). In addition, conventional autoradiography was performed.

Nuclear run-on analysis. Studies were performed as described previously (20). Briefly, confluent VT-treated and untreated BAEC cultures were washed with sterile 10 mM PBS and lysed in situ with chilled lysis buffer (10 mM Tris-HCl [pH 7.9], 0.15 M NaCl, 1 mM EDTA, and 0.6% [vol/vol] Nonidet P-40) for 10 min on ice. Cell lysates were centrifuged for 5 min at 500 *g* at 4°C, and the nuclear pellet resuspended in 75 μl of chilled nuclear buffer containing 0.3 M $(NH_4)_2SO_4$, 100 mM Tris-HCl (pH 7.9), 4 mM $MgCl_2$, 4 mM $MnCl_2$, 0.2 M NaCl, 0.4 mM EDTA, 0.1 mM PMSF, and 40% (vol/vol) glycerol. 100 μl of 1× cold transcription buffer (0.3 M $(NH_4)_2SO_4$, 100 mM Tris-HCl [pH 7.9], 4 mM $MgCl_2$, 4 mM $MnCl_2$, 0.2 M NaCl, 0.4 mM

EDTA, and 0.1 mM PMSF) containing 0.2 mM DTT, 40 U RNasin, 0.2 mM ATP, CTP, and GTP, and 150 μCi [α-^{32}P]UTP (3,000 Ci/mmol) was added to the nuclear suspension, and incubated for 30 min at 28°C. 20 U of RNase-free DNase 1 and 125 μg tRNA were added and incubated for 10 min at 37°C, followed by digestion with proteinase K at a final concentration of 300 μg/ml in buffer (10 mM Tris-HCl, pH 7.9, 10 mM EDTA, 0.5% SDS) for 30 min at 42°C. Nuclear transcripts were then extracted as described above and resuspended at 2×10^6 cpm/ml in Northern hybridization buffer. Equal amounts (1 μg) of gel-purified cDNA were denatured by boiling in 0.4 M NaOH-10-mM EDTA and neutralized with equal volumes of 2 M ammonium acetate, pH 7.0 (26), and slot-blotted onto nitrocellulose filters. The cDNA slot-blotted was identical to that used to generate the probes for Northern blot analysis. Hybridization was performed for 48–72 h at 42°C in Northern hybridization buffer as detailed above. Hybridized filters were washed as described (20), and subjected to autoradiography using a PhosphorImager (Molecular Dynamics) and quantitative densitometry assisted by the Molecular Dynamics ImageQuant Software package.

Actinomycin D chase experiments. To assess the effect of VT on the half-life of preproET-1 mRNA transcripts, confluent BAEC monolayers were treated with VT at 5 nM for 20 h before addition of 10 μg/ml actinomycin D. Previous studies demonstrated that the incorporation of [^{3}H]uridine into TCA-insoluble material was inhibited 99.5% by this treatment (31). Total cellular RNA was extracted at 0, 15, 30, 60, 120, and 180 min after the addition of actinomycin D. Blots were reprobed with an 18S rRNA-cDNA probe to ensure equal loading. PreproET-1 mRNA transcript levels were normalized for 18S rRNA using ImageQuant (Molecular Dynamics) and mRNA decay rates determined according to the formula: $N_t = N_0\, e^{-\lambda t}$. Results were from three independent experiments.

Protein extraction and immunoblotting. Confluent BAEC monolayers were lysed in situ with Laemmli buffer (62.5 mM Tris-HCl [pH 7.4], 2% [wt/vol] SDS, 10% [vol/vol] glycerol, and 0.72 M 2-mercaptoethanol), and total cellular protein extracted as described previously (20). Cell lysates were cleared at 100,000 *g* for 30 min at 25°C and stored at −80°C before analysis. The protein was quantitated using the modified Bradford method with bovine serum albumin as standard. 20 μg of protein was electrophoresed under reducing and denaturing conditions in 6% polyacrylamide gels. Equal loading was confirmed by replicate gel staining with Coomassie blue. Proteins were transferred to nitrocellulose filters using an electroblotting apparatus (Bio-Rad). Filters were blocked overnight at 4°C with 4% bovine serum albumin in Tris-buffered saline with 0.1% Tween 20, followed by a 2-h incubation at room temperature with a primary mouse monoclonal IgG antibody to human ecNOS which also recognizes bovine ecNOS (20) at a concentration of 0.125 μg/ml. Bound primary antibody was detected using horseradish-conjugated sheep anti–mouse IgG antibody diluted 1:20,000 for 1 h at room temperature followed by enhanced chemiluminescence substrate and brief exposure to autoradiographic films.

Endothelin radioimmunoassay. Confluent BAECs were exposed to VT2 at various concentrations for 24 h in serum-free culture medium in 24-well dishes. Conditioned medium (triplicate wells) was extracted over SepPak C18 cartridges, eluted with methanol-H_2O-acetic acid (90:9.6:0.4), lyophilized, and stored at −80°C until analysis with a radioimmunoassay kit specific for ET 1–21 as described previously (20). Cross-reactivity with big ET-1 was < 0.4%. While the assay cross-reacts with ET-2 and ET-3, ET-1 is the only isoform known to be produced by vascular endothelial cells (32). Levels of immunoreactive peptides are therefore taken to reflect production of ET-1. The intra- and interassay coefficients of variation averaged 6 and 10%, respectively. Cell numbers were assessed in representative wells using an automated cell counter (triplicate determinations).

Measurement of NO synthase activity. L-[^{14}C]citrulline conversion was determined using previously published methods with minor modifications (33, 34). Briefly, confluent cell monolayers grown in 6-well dishes were treated with VT2 at 4 or 0.1 nM or vehicle for 24 h as described above, gently rinsed with a physiologic salt solution (130 mM NaCl, 5 mM KCl, 1.5 mM $CaCl_2$, 1 mM $MgCl_2$, 25 mM Hepes [pH 7.4] and 10 mM D-glucose) equilibrated in 1 ml of the same buffer for 30 min at 37°C and labeled with $\sim 0.5 \times 10^6$ cpm/ml TLC-purified L-[^{14}C]arginine for 30 min. Cells were treated with 5 μM ionomycin or vehicle for the final 20 min at 37°C. The reaction was stopped with 4 ml of chilled 10 mM PBS/5 mM EDTA, pH 7.6. Cells were extracted with 1 ml of 0.3 M $HClO_4$ for 20 min at 4°C. Extracts were neutralized with 1 M K_2CO_3 and loaded onto a 1-ml wet bed volume of Dowex AG 50WX-8 cation exchange resin followed by 2 ml of water. L-[^{14}C]citrulline in the column effluent was quantitated by scintillation counting. TLC resolution of fractions of the column effluents and quantitation with the PhosphorImager indicated that L-[^{14}C]citrulline was the only detectable product. Counts (cpm) eluted from each resin column were normalized to total protein content and cell number per well.

Measurement of NO release. Basal and calcium-stimulated NO release was measured with chemiluminescence as described previously (35, 36) with minor modifications. Confluent monolayers grown in 6-well dishes treated with 5 nM VT2 for 24 h were gently rinsed with PBS containing 1.5 mM $CaCl_2$, and equilibrated in 0.6 ml of the same buffer at 37°C for 20 min before adding 5 μM ionomycin or vehicle. The conditioned buffer was removed at various time intervals (5–30 min) after the addition of ionomycin or vehicle and immediately frozen for storage at −80°C. To measure cell-released NO/NO_2^-, a rapid-response, ozone chemiluminescence analyzer was used (Model 280; Sievers, Boulder, CO). NO_2^- was reduced to NO in the presence of glacial acetic acid and excess NaI, and purged from solution with inert gas allowing mass-sensitive chemiluminescence detection based on the reaction of the NO radical with ozone (O_3). Manufacturer-specified lower limit of sensitivity for this analyzer was ~ 1 pmol of NO_2^- or NO injected into the purge vessel. The amount of released NO was derived from a standard curve of $NaNO_2$ (0.1–100 μM). Inter- and intraassay coefficient of variation was < 12% (36).

Data analysis. Data are expressed as means±SEM obtained in at least three separate experiments, unless indicated otherwise. Statistical analysis for paired comparisons was carried out using the Student's *t* test, and one-way ANOVA for serial determinations. The level of significance was defined as $P < 0.05$.

Results

Effect of VTs on endothelial metabolism. Confluent monolayers of BAECs were treated with VT1 and VT2 for 24 h at toxin concentrations ranging from 0.01 to 100 nM. The incorporation of [^{3}H]thymidine, [^{3}H]uridine, or [^{3}H]leucine was utilized

Table I. Concentration-dependent Effects of VTs and Ricin on Metabolite Incorporation Rates of BAECs

	IC_{50} (nM)			
Toxin	[^{3}H]Thymidine	[^{3}H]Uridine	[^{3}H]Leucine	*P**
VT1	6.6±1.0	104±3.3	55±7.3	< 0.005
VT1 B subunit	> 100	> 100	> 100	NS
VT2	4.0±0.6	102±10	53±15	< 0.005
Ricin (RCA_{60})	0.012±0.004	0.049±0.006	0.012±0.003	< 0.005

Confluent cell monolayers were exposed to toxin for 24 h before harvesting. Radiolabeled metabolites (1 μCi/well) were added during the final hour. Values are means±SEM, $n = 3$ experiments, triplicate determinations. *Differences between incorporation rates of metabolites (one-way ANOVA).

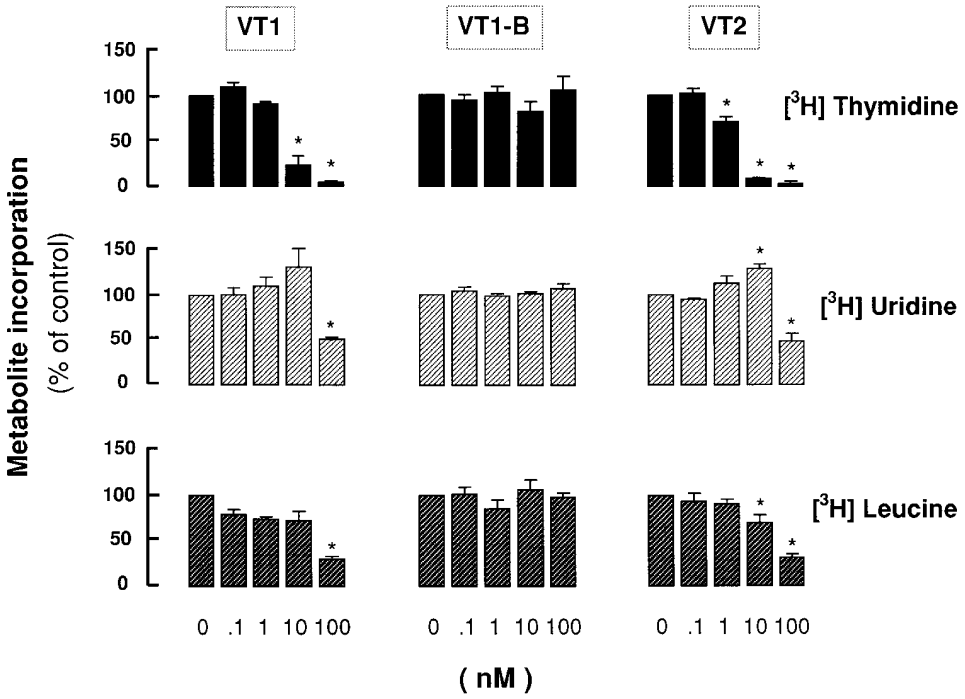

Figure 1. VT effects on global indices of endothelial cell metabolism. Confluent, serum-starved BAECs were exposed for 24 h to the indicated toxin concentrations and for 1 h to 1 μCi of [^{3}H]thymidine, [^{3}H]uridine, or [^{3}H]leucine. Radioactivity incorporated into TCA-insoluble material was determined. Data have been normalized to vehicle-treated cells. Shown are the means±SEM, $n = 3$ experiments, triplicate determinations. When error bars are not present, the SE was too small to appear. * Values significantly different from vehicle-treated BAECs.

to assess overall rates of synthesis of nascent DNA, RNA, and peptides, respectively. As shown in Fig. 1, at the highest toxin concentrations, incorporation of all metabolites was significantly reduced. 50% inhibitory concentrations (IC_{50}) are summarized in Table I. For VT2, likely the more important VT in human disease based on epidemiological data (37, 38), IC_{50} values for [^{3}H]thymidine, [^{3}H]uridine, and [^{3}H]leucine averaged 4.0±0.6, 102±10, and 53±15 nM, respectively. As shown in Fig. 1 and Table I, IC_{50} values for VT1 and VT2 on DNA, RNA, and peptide synthesis rates were quantitatively different in that more robust effects on inhibition of DNA synthesis were evident. VT1 and VT2 inhibited [^{3}H]thymidine incorporation at concentrations that were 1 to 2 log orders lower than those that reduced [^{3}H]leucine incorporation ($P < 0.01$ and < 0.05, respectively). In addition, the rate of [^{3}H]uridine incorporation was slightly increased at VT1 and VT2 concentrations

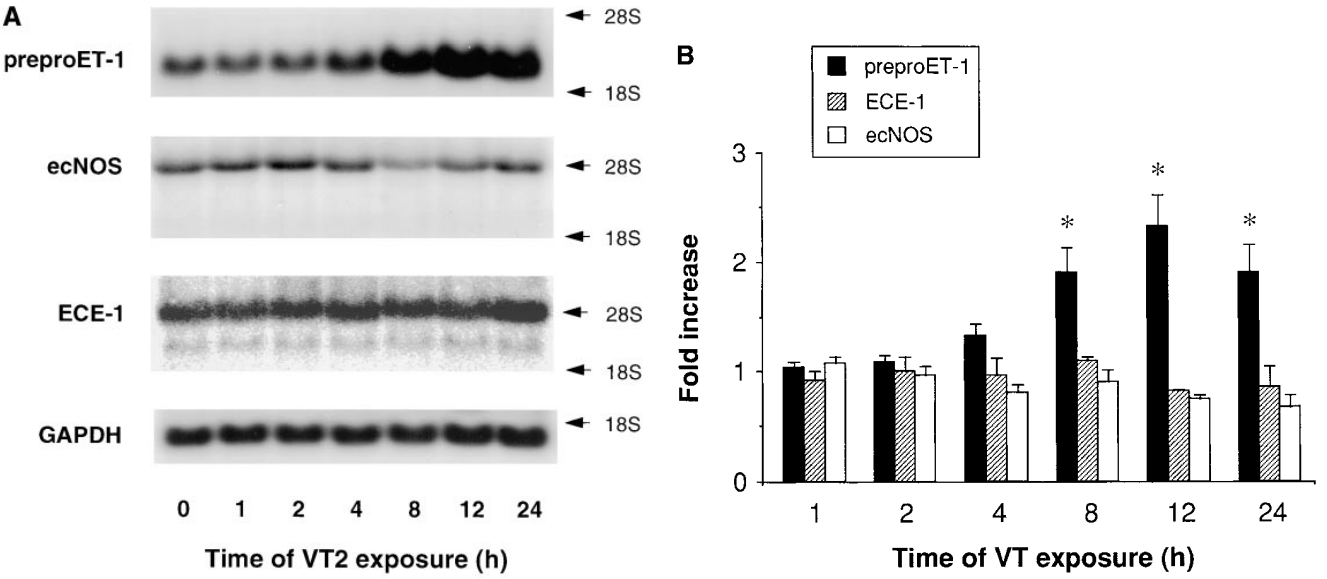

Figure 2. Time-dependent effect of VT2 on BAECs. Northern blot analysis (15 μg/lane) of total cellular RNA from BAECs treated with VT2 (8 nM) for the indicated time periods before harvest. Membranes were hybridized with [^{32}P]dCTP-labeled bovine preproET-1, ecNOS and with ECE-1 cDNA. GAPDH was used for reference. Blots were stripped between hybridizations. Radioactive signals were quantitated using ImageQuant software (Molecular Dynamics). (*A*) A representative blot is shown from four independent experiments with VT2. Similar results were obtained with VT1. (*B*) Densitometric analysis of blots from four independent experiments normalized to GAPDH and displayed as fold increase over untreated controls. * Values significantly different from vehicle-treated BAECs.

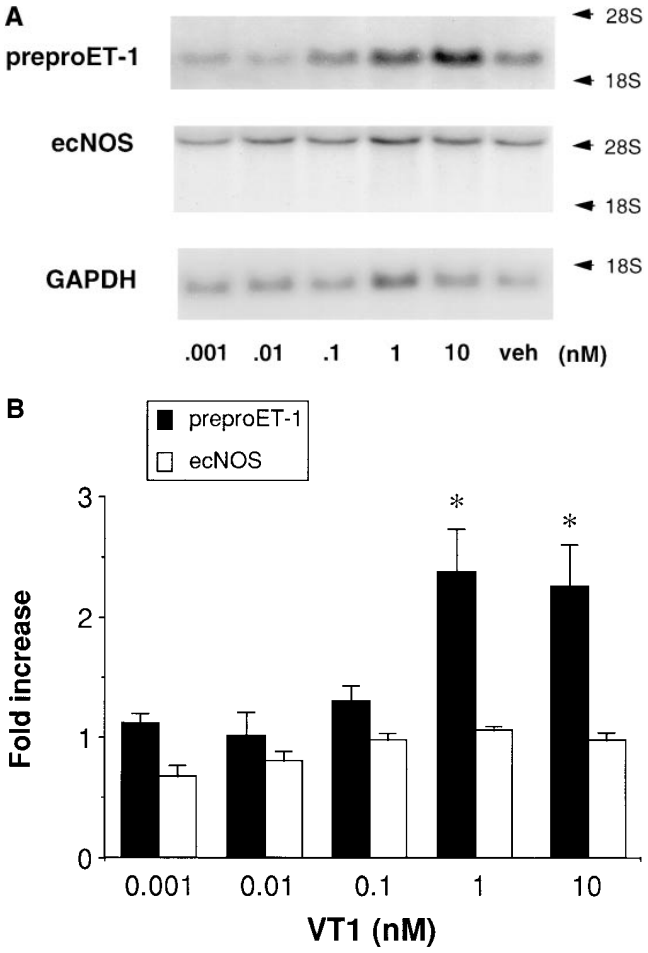

Figure 3. Concentration-dependent effect of VT2 on BAECs. Northern blot analysis of total cellular RNA (15 μg/lane) from BAECs exposed for 24 h to the indicated concentrations of VT1. Blots were hybridized with [^{32}P]dCTP-labeled preproET-1 cDNA, stripped, and reprobed for ecNOS and GAPDH. (*A*) A representative blot is shown from one of four independent experiments with VT1. (*B*) Densitometric analysis of blots from four independent experiments normalized to GAPDH and displayed as fold increase over baseline. *Values significantly different from control BAECs.

up to 20 nM (Fig. 1). VT1 B subunit, which lacks *N*-glycosidase activity, failed to modify DNA, RNA, and peptide synthesis (Fig. 1), suggesting that the A subunit is responsible for the observed biologic effects. VT2e, which utilizes a different glycosphingolipid receptor, namely Gb4, was significantly less active in BAECs than VT1 and VT2 up to concentrations of 100 nM (results not shown).

VTs increase preproET-1 steady-state mRNA levels. The effects of VT1 and VT2 on steady-state mRNA expression of preproET-1, ECE-1, and ecNOS in cultured endothelial cells was assessed by Northern analysis. Exposure to VT1 or VT2 induced a concentration- and time-dependent increase in 2.3-kb preproET-1 mRNA transcript levels in BAECs. Under these conditions, monolayers revealed little to no microscopic alterations compared with vehicle-treated controls. VT-induced increases in preproET-1 mRNA levels were evident after as early as 4 h, with maximal effects observed at 12–24 h (Fig. 2). Concentration–response relationships (0.001–10 nM) were assessed at 24 h and are shown in Fig. 3. The threshold concentration for increases in preproET-1 mRNA level was 0.5 nM for both VT1 and VT2 (Fig. 3 *B*). Concentrations between 1 and 10 nM, used in various independent experiments, caused a 2–3-fold increase in steady-state preproET-1 mRNA levels over GAPDH signals (VT1, 2.6±0.3-fold increase, mean±SE, $n = 7$; VT2, 2.2±0.2-fold, $n = 8$). These results indicate that increased preproET-1 transcript levels were observed at VT concentrations that had minor effects on overall protein synthesis and gene transcription (compare with Fig. 1). VT1 B subunit (1–10 nM) failed to change steady-state preproET-1 mRNA levels (Fig. 4).

Effect of VTs on ECE-1 and ecNOS mRNA expression. VT1 and VT2 holotoxins, and the VT1 B subunit failed to modify steady-state mRNA levels for ECE-1 and ecNOS at varied time points and concentrations (Figs. 2 and 3). These negative findings were confirmed with multiple independent BAEC clones ($n = 6$). Results of a representative experiment comparing the effects of relevant concentrations of VT1, VT2, and the VT1 B subunit on preproET-1 and ECE-1 mRNA transcript levels in BAECs are shown in Fig. 4.

Effect of VT2 on immunoreactive endothelin peptide secretion. Exposure of BAEC to 5 nM VT2 for 24 h increased the amount of secreted immunoreactive peptide as assessed with a highly specific radioimmunoassay at 5 nM (Fig. 5).

Effect of VT2 on ecNOS protein expression. Total cellular immunoreactive endothelial NOS protein in BAECs was assessed by Western blot studies. In protein extracts of cells under basal conditions a single immunoreactive band of ~135 kD was detected. Treatment of BAECs with VT2 (8 nM) for 24 or 48 h failed to have a significant effect on steady-state levels of immunoreactive ecNOS protein. A representative blot is shown in Fig. 6. Results were confirmed with six independent BAEC clones.

Measurement of NOS enzymatic activity. L-[^{14}C]arginine to L-[^{14}C]citrulline conversion was determined using quantitative cation-exchange chromatography as described previously (34).

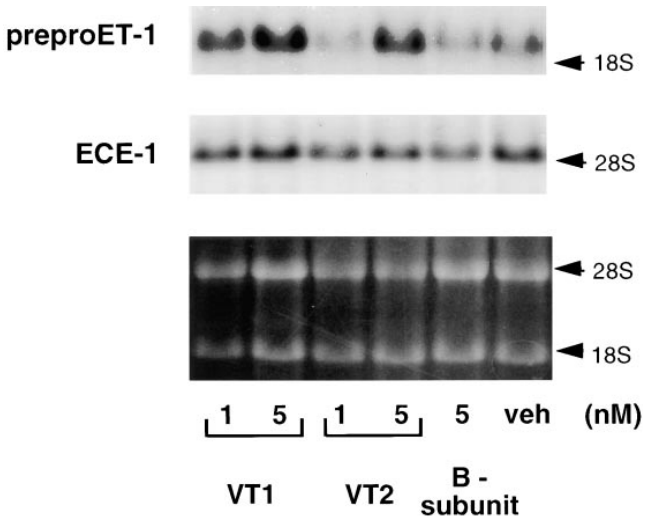

Figure 4. Comparative Northern blot analysis of total cellular RNA (10 μg/lane) isolated from BAECs treated with VT1, VT2, or VT1 B subunit toxins at the indicated concentrations for 24 h. cDNA probes were used as described in the legend to Fig. 2. The ethidium bromide–stained gel is included for documentation of RNA loading.

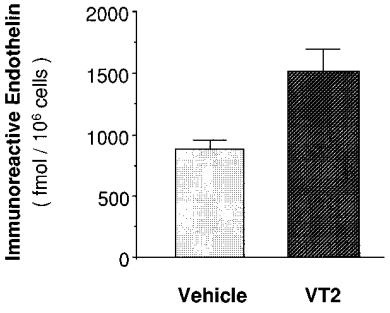

Figure 5. Measurement of immunoreactive endothelin in the conditioned medium of BAECs exposed to vehicle or VT2 at 5 nM for 24 h. Data represent mean±SE from one of two experiments (triplicate determinations).

Fig. 7 *A* shows the effect of VT2 (24 h; 0.1 and 4 nM) on BAECs L-[^{14}C]citrulline formation in the absence and presence of the calcium ionophore ionomycin (5 μM, 20 min). L-[^{14}C]citrulline formation increased in BAECs in response to ionomycin consistent with the observation that constitutive NOS activity in BAECs is calcium and calmodulin-dependent. Rates of L-[^{14}C]citrulline formation were not modified by VT2 in the absence or presence of ionomycin.

Effect of VT2 on NO chemiluminescence signal. NO release from BAEC monolayers was determined as [NO + NO_2^-] using a chemiluminescence detection method. Ionomycin (5 μM) treatment increased the chemiluminescence signal approximately threefold above vehicle-treated cells. Vehicle- and ionophore-stimulated release of NO/NO_2^- from BAECs was not altered by VT2 (24 h, 5 nM, $n = 3$) (Fig. 7 *B*).

Nuclear run-on studies. To define the molecular mechanism underlying the observed increase in preproET-1 steady-state mRNA levels after VT treatment, nuclear run-on studies were performed in BAECs exposed to VT2 (5 nM) for 6 or 24 h. cDNA probes reflecting 5′ and 3′ regions of the transcription units were used to assess potential effects on polymerase processivity (transcriptional arrest) (39) after VT treatment. Although hybridization of labeled, nascent nuclear RNA to 3′-cDNA probes for preproET-1 and ecNOS yielded weaker signals than hybridization to the 5′ probes of the same cDNA, no appreciable differences in the rate of transcription of preproET-1, ecNOS, and ECE-1 mRNA, or in polymerase processivity were noted between different treatment conditions (Fig. 8, *A* and *B*). Identical results were obtained when BAECs were exposed to equimolar concentrations of VT1 (not shown).

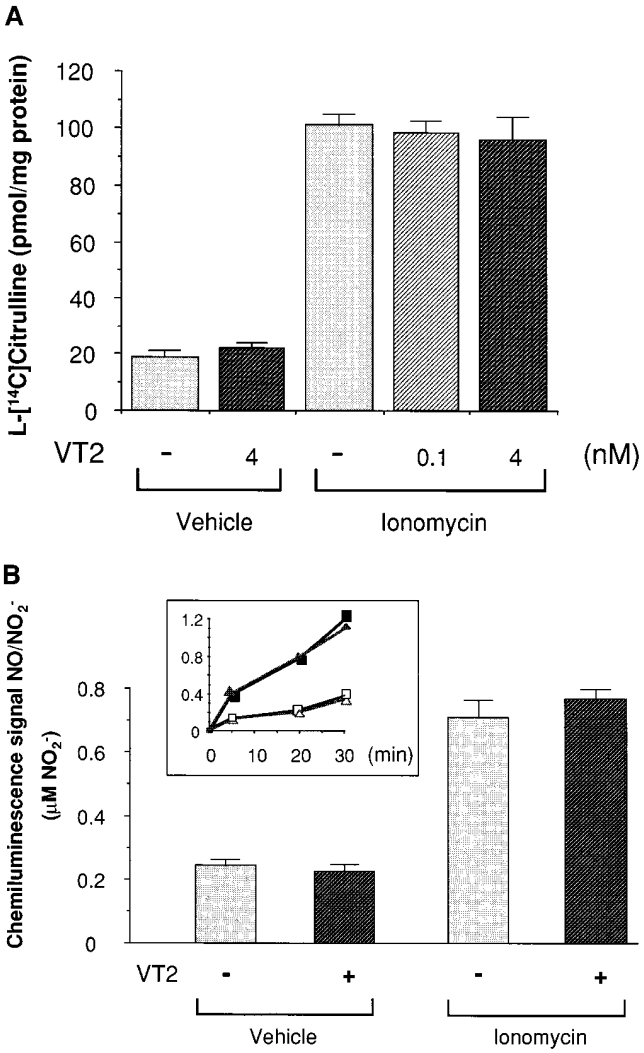

Figure 7. Effect of VT on NOS activity and NO/NO_2^- release from BAECs. (*A*) L-[^{14}C]arginine–L-[^{14}C]citrulline conversion. Confluent cell monolayers were exposed to vehicle or VT2 at the indicated concentrations for 24 h. 1 h before harvesting, culture medium was replaced by a physiologic salt solution containing 0.5×10^6 cpm/well L-[^{14}C]arginine and then treated with vehicle or ionomycin (5 μM, 20 min). After extraction with ice-cold $HClO_4$, L-[^{14}C]arginine was determined by quantitative cation-exchange chromatography. Bars represent the mean±SEM of three experiments (triplicate determinations). (*B*) Chemiluminescence determination of NO/NO_2^-. Confluent monolayers were treated with 5 nM VT2 for 24 h. After replacement of culture medium with a physiological salt solution vehicle or ionomycin (5 μM) was added for 20 min. NO/NO_2^- content of conditioned salt solution was determined using chemiluminescence methodology. Results are presented from three independent experiments (mean±SE). Inset depicts the time course of a representative experiment (△, vehicle-treated cells; □, VT-treated, unstimulated cells; ▲, ionomycin-stimulated cells; ■, VT-treated, ionomycin-stimulated cells).

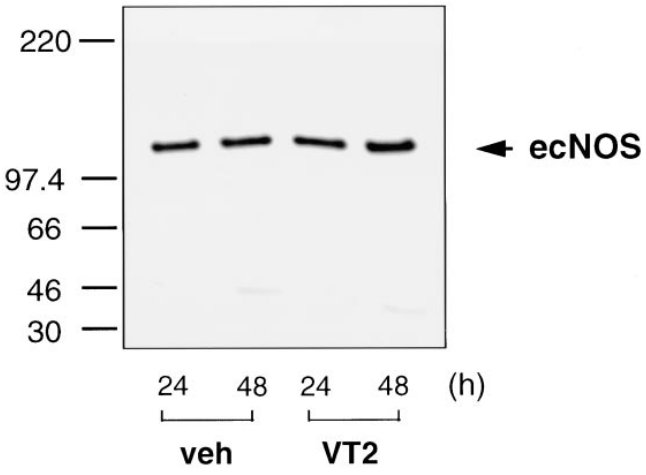

Figure 6. Effect of VT2 on immunoreactive ecNOS protein levels in BAECs. BAECs were exposed to vehicle or VT2 (8 nM) for 24 or 48 h. Immunoblotting was performed using 20 μg/lane of total cellular protein extract. Bovine immunoreactive protein was detected with an mAb for ecNOS. Data are representative of four independent experiments using six different BAEC clones.

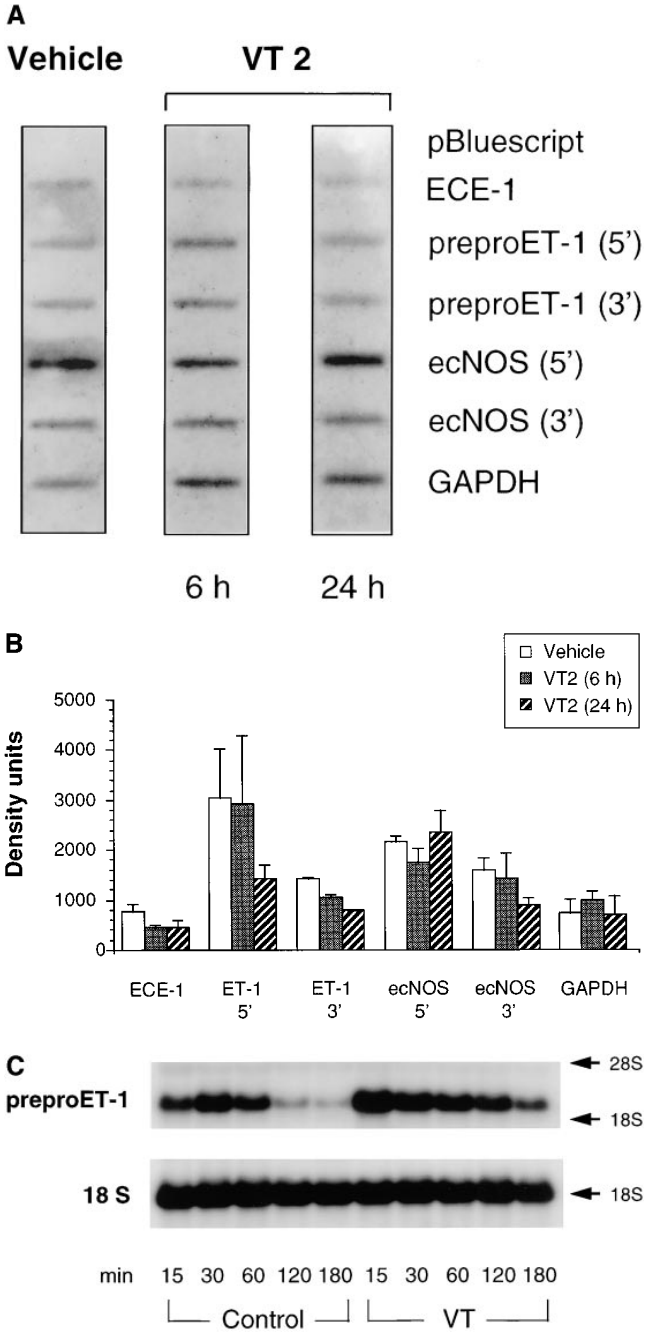

Figure 8. Molecular mechanism of VT-induced increases in steady-state preproET-1 mRNA levels. (*A*) Effect of vehicle or VT2 (5 nM; 0, 6, 24 h) on the rate of endothelial gene transcription. Isolated cell nuclei were allowed to generate nuclear run-on products in the presence of [^{32}P]UTP and then hybridized to linear, immobilized cDNA probes as indicated. PreproET-1 and ecNOS cDNA probes reflecting 3′ and 5′ regions of the transcription units were used to assess polymerase processivity after VT treatment. There were no significant differences in signal strength between vehicle and VT2-treated BAECs. (*B*) Quantitative densitometry of the results of three independent nuclear run-on experiments. Data represent mean±SE from three independent experiments. (*C*) Representative Northern blot (15 μg/lane) analysis of the rate of disappearance of preproET-1 mRNA in BAECs after transcriptional blockade at time 0 with actinomycin D (10 μg/ml). Confluent monolayers were treated with VT (5 nM) or vehicle, 20 h before the addition of actinomycin D. Total cellular RNA was extracted at various time points after addition of actinomycin D. Blots were rehybridized with an 18S ribosomal RNA probe to correct for loading differences between lanes. The half-life for preproET-1 mRNA was calculated from three independent experiments and averaged 35±2 and 86±23 min (mean±SE) for vehicle- and VT-treated cells, respectively ($P < 0.05$).

Actinomycin D chase experiments. BAECs were treated with a potent transcriptional inhibitor, actinomycin D, allowing quantitation of the rate of preproET-1 mRNA decay. Fig. 8 *C* shows a representative Northern blot of one of three independent actinomycin D chase experiments. Confluent monolayers, pretreated for 20 h with 5 nM VT or vehicle received actinomycin D (10 μg/ml) at time 0. Total cellular RNA was extracted 15–180 min after addition of actinomycin D. Analysis of densitometric data revealed that VT increased the half-life of preproET-1 mRNA in BAECs on average by 2.5-fold, from 35±2 to 86±23 min ($n = 3$; $P < 0.05$). These findings, in concert with the nuclear run-on studies, indicated that the observed increase in preproET-1 mRNA transcript levels in vascular endothelial cells was not due to increased rates of transcription but solely due to changes in mRNA degradation: specifically, VTs prolong the mRNA half-life of preproET-1.

The effect of ricin on endothelial metabolism and preproET-1 steady-state mRNA levels. The plant protein toxin ricin shares with VTs the ability, via its structurally related A subunit, to depurinate 28S rRNA at the identical site (16). However, VTs and ricin display differences in receptor specificity and intracellular transport (40). To gain further insight into the biologic effects of ribosome inactivating proteins in endothelial cells, we examined the effects of ricin on basal rates of DNA, RNA, and protein synthesis and on preproET-1 mRNA steady-state levels in BAECs. As shown in Table I, ricin inhibited [^{3}H]leucine incorporation at a concentration 3 log orders below those of VT1 and VT2 (IC_{50} 12±3 pM vs. > 50 nM). Furthermore, ricin significantly elevated the incorporation of [^{3}H]uridine at 10 pM (Fig. 9 *A*). Ricin increased preproET-1 mRNA transcript levels in a time- (not shown) and concentration-dependent manner (1.8±0.2-fold and 5.1±1.0-fold at 1 and 10 pM, respectively; $n = 8$) (Fig. 9 *B*), and, similar to VT1 and VT2, failed to modify ecNOS and ECE-1 mRNA transcript levels (not shown).

Discussion

In this study, we determined the effect of VTs on the expression of the endothelial vasomediators, ET-1 and NO, and their key regulatory enzymes, ECE-1 and ecNOS. The major finding was the ability of VT1 and VT2 to increase preproET-1 steady-state mRNA levels in vascular endothelium in a time- and concentration-dependent manner. Importantly, the VT effect on preproET-1 mRNA levels was observed at concentrations that had minor effects on global nascent peptide synthesis, and therefore does not appear to be a consequence of generalized ribosomal blockade. Furthermore, the concentration of VT2 used did not diminish the release of immunoreactive endothelin in conditioned medium, but rather increased the amount of immunoreactive peptide. In contrast to preproET-1, mRNA transcript levels of the membrane-bound metalloprotease ECE-1, a key enzyme in the biosynthesis pathway of the endothelins, were not modified by VT1 or

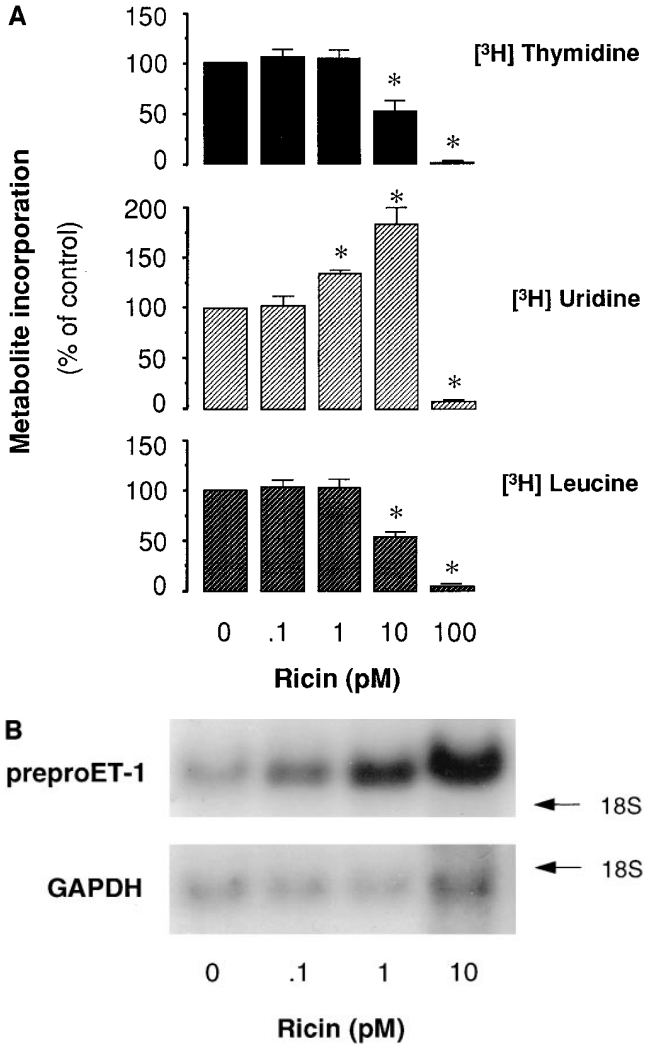

Figure 9. Ricin effect on BAECs. (*A*) Confluent cells were exposed for 24 h to the indicated toxin concentrations, pulse-labeled for 1 h with [^{3}H]thymidine, [^{3}H]uridine, or [^{3}H]leucine (1 μCi/0.5 ml medium), and harvested as described in the legend to Fig. 1. Results from three independent triplicate experiments normalized to untreated controls are shown (mean±SE). * Values significantly different from vehicle-treated BAECs. (*B*) Northern blot analysis of ricin concentration–response relationship measured at 24 h. Total RNA was extracted from BAECs monolayers, size-fractionated (7.5 μg/lane), and hybridized with [^{32}P]-labeled cDNA for preproET-1 or GAPDH as reference probe.

VT2. Our novel observation that VTs induce preproET-1 expression in the absence of exogenous cytokines suggests that VT1 and VT2 can activate endothelial cells directly. We take these data to indicate that activation of endothelial cells by VTs is an important biological function of this family of toxins.

We originally hypothesized that modulation of NO production may play a role in the pathogenesis of VT-induced thrombotic microangiopathy. Endothelial-derived NO is known to prevent platelet activation (18). For example, rats injected with LPS and the NOS inhibitor L-NAME evidence thrombotic microangiopathy in the kidney: glomerular capillary thrombosis was observed in > 50% of the glomeruli examined, whereas < 5% of the glomeruli were affected in rats receiving LPS or L-NAME alone (41). That VTs may act, in part, by impairing ecNOS expression or activity was an attractive hypothesis. However, VT2 failed to modify steady-state ecNOS mRNA or immunoreactive protein levels and calcium-stimulated L-[^{14}C]arginine to L-[^{14}C]citrulline conversion rates or NO/NO_2^- release in BAECs under in vitro conditions.

To what extent are VT-induced increases in preproET-1 mRNA and protein relevant in the pathophysiological context? Increased preproET-1 may contribute directly or indirectly to the vasculopathy associated with VTs. Endothelins are produced by, bind to, and stimulate biologic processes in various tissues and cell types in an autocrine and paracrine fashion (32, 42). Relevant pathophysiological features of HUS and hemorrhagic colitis, such as severe hypertension (9, 43), and focal ischemia of renal cortex (6–8), gut mucosa (ischemic colitis, hemorrhage) (3, 7, 44), and the central nervous system (seizures, stroke) (45, 46) are compatible with VT-mediated production of this potent vasoconstrictor. Although the synthesis of paracrine and autocrine mediators is poorly reflected by their plasma or urine levels, especially in the setting of impaired renal function, it is interesting to note that children with VT-associated HUS demonstrated increased urinary concentrations of ET-1 (47). The renal vasculature appears to be exquisitely sensitive to ET-1. ET-1 can potently activate a cascade of signaling events in glomerular mesangial cells, that culminates in a contractile, proliferative, and secretory phenotype (42). For instance, ET-1 may elicit autoinduction of ET-1 secretion in these cells (42, 48). Taken as a whole, a number of studies have implicated ET-1 in diverse aspects of acute renal failure. For example, studies utilizing ET_A and ET_B receptor antagonists have demonstrated an important role for ET-1 in ischemia/reperfusion injury in the kidney, and acute cyclosporine nephrotoxicity, among others (42, 49, 50). Moreover, endothelin-mediated vasoconstriction can reduce cerebral blood flow causing ischemic neuronal injury and induce neurotoxicity (51). In the gut, ET-1 can induce ischemia and mucosal damage (52, 53), disturb ion transport, and elicit contractions of nonvascular smooth muscle, especially in the colon wall (54, 55). Under certain conditions ET-1 may also exert prothrombotic effects (56). Future studies assessing expression of preproET-1 mRNA in animal models of verotoxemia are warranted in order to support the biologic significance of our in vitro findings.

The human preproET-1 gene has been used as a prototypic gene in defining the basic principles governing constitutive gene transcription in vascular endothelium. Reporter-promoter gene constructs have identified GATA-2 and AP1 *trans*-acting factors as quintessential in the functional activity of the proximal core ET-1 promoter (57). Superimposed upon these basal processes is the regulation of rates of transcription initiation by exogenous stimuli: shear stress, hypoxia, and inflammatory cytokines, such as TNF-α, LPS, and IL-1, among others (32). Studies on the metabolic fate of preproET-1 mRNA indicate that the transcript is very labile, with a half-life of ~ 15–30 min (30). In this study, VT-induced preproET-1 mRNA transcript accumulation in BAECs was detectable within 4–8 h, and maximal after 12–24 h of VT exposure. Actinomycin D chase experiments demonstrated that VTs increased the half-life of preproET-1 mRNA transcripts ~ 2.5-fold. Rates of preproET-1 gene transcription initiation and elongation were not affected. We take these data to indicate that the VTs increase steady-state mRNA levels for preproET-1 by

modifying the biological fate of the mRNA. This is a novel finding as preproET-1 was thought previously to be regulated in endothelial cells solely at the level of transcription initiation (31, 32). Interestingly, Iwasaki et al. (48) reported recently that in rat glomerular mesangial cells ET_B receptor–mediated autoinduction of ET-1 involves both increased rates of transcription and mRNA stability of preproET-1.

Understanding the biologic fates of mRNA transcripts is an exciting and fast developing field. Rapid decay of labile mRNA species has been ascribed to the presence of AU-rich ribonucleotide sequences, especially the UUAUUUA(U/A)(U/A) nonamer consensus element in the 3′ untranslated region (UTR) of mRNA transcripts (58, 59). Sequence inspection reveals that the human and bovine preproET-1 mRNAs contain several AU-rich elements. A nonconsensus, conserved nonamer sequence (AUAUUUAUA) (59) is present in the 3′-UTR of human and bovine preproET-1. We posit that the molecular basis of VT-induced increases in the mRNA half-life of endothelial preproET-1 mRNA transcripts involves VT-induced changes in interactions between RNA-binding proteins and *cis* elements of these transcripts, with subsequent alterations of their decay rates (60, 61). An alternative hypothesis, that is not mutually exclusive, suggests that VTs modulate translation-dependent mRNA degradation pathways in a transcript-specific fashion (61, 62). Clearly, further mechanistic insight into this novel effect of VTs on labile mRNAs is necessary. In this regard, preproET-1 will be a useful model. Recent studies on the effect of VTs on mouse peritoneal macrophages (63) and human peripheral blood monocytes (64, 65) indicate that VTs, at a concentration of 10 nM, enhanced the secretion of TNF-α and IL-1β via an LPS-independent pathway (64, 65). These cytokines are also encoded by labile mRNA transcripts (59). In the above studies, the monocytic cells were resistant to protein synthesis inhibition at the VT concentrations used. In mice transgenic for a TNF-α promoter chloramphenicol acetyltransferase reporter gene, VT increased chloramphenicol acetyltransferase activity in kidney homogenates (66). The design of this insertional transgene, which contained both 5′-flanking sequences and the complete TNF-α 3′-UTR with its consensus nonamer AU-rich element, precludes comments with respect to the relative contributions of transcription or RNA stability. Taken together, it is plausible that VTs modulate the biologic fate of a unique population of mRNA species and that this phenomenon plays a prominent role in the pathophysiology of endothelial activation.

The extremely potent cytotoxicity of ricin for mammalian cells has been documented in a publicized homicide case (67). The therapeutic utility of ricin and, more recently, of VT1 in malignancies (15, 68) has stimulated interest in the specific pathways involved in ribosome-inactivating proteins and protein–rRNA interaction (14, 17, 69, 70). Here we describe a model of endothelial activation by ricin. This toxin exhibited potent effects on endothelial phenotype at picomolar concentrations, i.e., three log orders lower than VT1 and VT2. Ricin is efficiently internalized via clathrin-dependent and -independent receptor-cycling pathways utilizing β-D-galactopyranoside and *N*-acetyl-D-galactosamine moieties of membrane glycolipids and glycoproteins (69). The differential sensitivity of BAECs to the biologic effects of VTs and ricin may be related to the abundance of receptors required for the intracellular (retrograde) transport of these toxins (13, 14). Indeed, we found that BAECs contain significantly less Gb3 than Vero cells (6.4±1.2 vs. 272 pmol/10^6 cells) and no detectable Gb4 (HPLC measurement of independent BAEC clones; data not shown). Nevertheless, both VT and ricin demonstrated a similar increase in preproET-1 mRNA levels in BAECs at concentrations that had marginal effects on [^{3}H]leucine incorporation (Figs. 1 and 9). In view of the similarity of the enzymatic action of VT and ricin A chains, our results suggest a major role for the A subunit in the observed biologic effects in endothelial cells.

Recent work indicates that ricin and certain classes of peptide synthesis inhibitors (e.g., anisomycin) activate stress-activated protein kinases (or c-Jun NH_2-terminal kinases) at concentrations that do not affect rates of global peptide synthesis (71). The relationship between these observations, as well as the signaling cascades relevant to the effects of VTs and ricin on overall rates of [^{3}H]uridine and [^{3}H]thymidine incorporation at sublethal concentrations remains to be determined. We posit that enzymatic modification of the A^{4324} residue of the 28S rRNA subunit by VTs or ricin elicits an intriguing change in cellular signaling cascades that impinges on the degradation pathway(s) of select mRNAs. This pathway is activated by toxin concentrations that are below those necessary for their well characterized inhibitory effects on nascent peptide synthesis. The pathway likely operates via *cis*-RNA elements in the preproET-1 transcripts, possibly the 3′-UTR.

Taken together, these studies indicate that VTs and ricin possess novel regulatory and cell-activating effects at concentrations that are below their inhibitory effects on de novo peptide synthesis. These effects may be of particular relevance for our understanding of the pathogenesis and pathophysiology of VT-mediated disease, especially HUS.

Acknowledgments

We thank M.A. Karmali for preparations of VT1 and VT2; C.A. Lingwood and G.J. Tyrrell for VT2e; J.L. Brunton for VT1 B subunit; K. Ludwig, M. Winkler, and D.J. Bast for assistance with toxin purification; B. Boyd for glycolipid measurements; and N. Zamel, P.E. Silkoff, and S. Dai for help with NO measurements.

M.M. Bitzan is the recipient of a Dyson Research Fellowship and Kidney Foundation of Canada Award. Y. Wang is the recipient of a Medical Research Council of Canada Fellowship Award. P.A. Marsden is the recipient of a Medical Research Council of Canada Scholarship and is supported by grant GR-13298 from the Medical Research Council of Canada.

References

1. O'Brien, A.D., V.L. Tesh, A. Donohue-Rolfe, M.P. Jackson, S. Olsnes, K. Sandvig, A.A. Lindberg, and G.T. Keusch. 1992. Shiga toxin: biochemistry, genetics, mode of action, and role in pathogenesis. *Curr. Top. Microbiol. Immunol.* 180:65–94.

2. Karmali, M.A., B.T. Steele, M. Petric, and C. Lim. 1983. Sporadic cases of hemolytic uremic syndrome associated with fecal cytotoxin and cytotoxin-producing *Escherichia coli. Lancet.* 1:619–620.

3. Riley, L.W., R.S. Remis, S.D. Helgerson, H.B. McGee, J.G. Wells, B.R. Davis, R.J. Hebert, E.S. Olcott, L.M. Johnson, N.T. Hargrett, et al. 1983. Hemorrhagic colitis associated with a rare *Escherichia coli* serotype. *N. Engl. J. Med.* 308:681–685.

4. Tarr, P.I. 1995. *Escherichia coli* O157:H7. Clinical, diagnostic, and epidemiological aspects of human infection. *Clin. Infect. Dis.* 20:1–10.

5. Linggood, M.A., and J.M. Thompson. 1987. Verotoxin production among porcine strains of *Escherichia coli* and its association with oedema disease. *J. Med. Microbiol.* 25:359–362.

6. Habib, R., M. Levy, M.F. Gagnadoux, and M. Broyer. 1982. Prognosis of the hemolytic uremic syndrome in children. *Adv. Nephrol.* 11:99–128.

7. Richardson, S.E., M.A. Karmali, L.E. Becker, and C.R. Smith. 1988. The

histopathology of the hemolytic uremic syndrome associated with Verocytotoxin-producing *Escherichia coli* infections. *Hum. Pathol.* 19:1102–1108.

8. Argyle, J.C., R.J. Hogg, T.J. Pysher, F.G. Silva, and R.L. Siegler. 1990. A clinicopathological study of 24 children with hemolytic uremic syndrome. *Pediatr. Nephrol.* 4:52–58.

9. O'Brien, J.A., S.K. van Why, M.S. Keller, K.M. Gaudio, T.L. Kennedy, and N.J. Siegel. 1994. Altered renovascular resistance after spontaneous recovery from hemolytic uremic syndrome. *Yale J. Biol. Med.* 67:1–14.

10. Bergstein, J.M., M. Riley, and N.U. Bang. 1992. Role of plasminogen-activator inhibitor type 1 in the pathogenesis and outcome of the hemolytic-uremic syndrome. *N. Engl. J. Med.* 327:755–759.

11. Benigni, A., and G. Remuzzi. 1994. The role of eicosanoids in the pathogenesis of hemolytic uremic syndrome. *Prostaglandins Leukot. Essent. Fatty Acids.* 51:75–79.

12. Remuzzi, G., and P. Ruggenenti. 1995. The hemolytic uremic syndrome. *Kidney Int.* 47:2–19.

13. Lingwood, C.A. 1993. Verotoxins and their glycolipid receptors. *Adv. Lipid Res.* 25:189–211.

14. Sandvig, K., M. Ryd, O. Garred, E. Schweda, P.K. Holm, and B. van Deurs. 1994. Retrograde transport from the Golgi complex to the ER of both Shiga toxin and the nontoxic Shiga B-fragment is regulated by butyric acid and cAMP. *J. Cell Biol.* 126:53–64.

15. Lord, J.M., L.M. Roberts, and J.D. Robertus. 1994. Ricin: structure, mode of action, and some current applications. *Fed. Am. Soc. Exp. Biol. J.* 8: 201–208.

16. Furutani, M., K. Kashiwagi, K. Ito, Y. Endo, and K. Igarashi. 1992. Comparison of the modes of action of a Vero toxin (a Shiga-like toxin) from *Escherichia coli*, of ricin, and of alpha-sarcin. *Arch. Biochem. Biophys.* 293:140–146.

17. Wool, I.G., A. Glück, and Y. Endo. 1992. Ribotoxin recognition of ribosomal RNA and a proposal for the mechanism of translocation. *Trends Biochem. Sci.* 17:266–269.

18. Radomski, M.W., R.M.J. Palmer, and S. Moncada. 1987. Endogenous nitric oxide inhibits human platelet adhesion to vascular endothelium. *Lancet.* 2:1057–1058.

19. Marsden, P.A., and B.M. Brenner. 1991. Nitric oxide and endothelins: novel autocrine/paracrine regulators of the circulation. *Semin. Nephrol.* 11:169–185.

20. Flowers, M.A., Y. Wang, R.J. Stewart, B. Patel, and P.A. Marsden. 1995. Reciprocal regulation of endothelin-1 and endothelial constitutive NOS in proliferating endothelial cells. *Am. J. Physiol.* 269:H1988–H1997.

21. Petric, M., M.A. Karmali, S. Richardson, and R. Cheung. 1987. Purification and biological properties of *Escherichia coli* verocytotoxin. *FEMS Microbiol. Lett.* 41:63–68.

22. Downes, F.P., T.J. Barrett, J.H. Green, C.H. Aloisio, J.S. Spika, N.A. Strockbine, and I.K. Wachsmuth. 1988. Affinity purification and characterization of Shiga-like toxin II and production of toxin-specific monoclonal antibodies. *Infect. Immun.* 56:1926–1933.

23. Ramotar, K., B. Boyd, G. Tyrrell, J. Gariepy, C. Lingwood, and J. Brunton. 1990. Characterization of Shiga-like toxin I B subunit purified from overproducing clones of the SLT-I B cistron. *Biochem. J.* 272:805–811.

24. Richardson, S.E., T.A. Rotman, V. Jay, C.R. Smith, L.E. Becker, M. Petric, N.R. Olivieri, and M.A. Karmali. 1992. Experimental verocytotoxemia in rabbits. *Infect. Immun.* 60:4154–4167.

25. Marsden, P.A., T.A. Brock, and B.J. Ballermann. 1990. Glomerular endothelial cells respond to calcium-mobilizing agonists with release of EDRF. *Am J. Physiol.* 258:F1295–F1303.

26. Sambrook, J., E.F. Fritsch, and T. Maniatis. 1989. Molecular Cloning: A Laboratory Manual. Cold Spring Harbor Laboratory Press, Cold Spring Harbor, NY.

27. Lamas, S., T. Michel, T. Collins, B.M. Brenner, and P.A. Marsden. 1992. Effects of interferon-gamma on nitric oxide synthase activity and endothelin-1 production by vascular endothelial cells. *J. Clin. Invest.* 90:879–887.

28. Lamas, S., P.A. Marsden, G.K. Li, P. Tempst, and T. Michel. 1992. Endothelial nitric oxide synthase: molecular cloning and characterization of a distinct constitutive enzyme isoform. *Proc. Natl. Acad. Sci. USA.* 89:6348–6352.

29. Oberbäumer, I.A. 1992. Retroposons do jump: a B2 element recently integrated in an 18S rDNA gene. *Nucl. Acids Res.* 20:671–677.

30. Marsden, P.A., D.M. Dorfman, T. Collins, B.M. Brenner, S.H. Orkin, and B.J. Ballermann. 1991. Regulated expression of endothelin 1 in glomerular capillary endothelial cells. *Am. J. Physiol.* 261:F117–F125.

31. Marsden, P.A., and B.M. Brenner. 1992. Transcriptional regulation of the endothelin-1 gene by TNF-α. *Am. J. Physiol.* 262:C854–C861.

32. Rubanyi, G.M., and M.A. Polokoff. 1994. Endothelins: molecular biology, biochemistry, pharmocology, physiology, and pathophysiology. *Pharmacol. Rev.* 46:325–415.

33. Bredt, D.S., and S.H. Snyder. 1989. Nitric oxide mediates glutamate-linked enhancement of cGMP levels in the cerebellum. *Proc. Natl. Acad. Sci. USA.* 86:9030–9033.

34. Lamas, S., T. Michel, B.M. Brenner, and P.A. Marsden. 1991. Nitric oxide synthesis in endothelial cells: evidence for a pathway inducible by TNF-alpha. *Am. J. Physiol.* 261:C634–C641.

35. Leone, A.M., P. Rhodes, V. Fürst, and S. Moncada. 1995. Techniques for the measurement of nitric oxide. *Methods Mol. Biol.* 41:285–299.

36. Silkoff, P.E., P.A. McClean, A.S. Slutsky, H.G. Furlott, E. Hoffstein, S. Wakita, K.R. Chapman, J.P. Szalai, and N. Zamel. 1997. Marked flow-dependence of exhaled nitric oxide using a new technique to exclude nasal nitric oxide. *Am. J. Respir. Crit. Care Med.* 155:260–267.

37. Ostroff, S.M., P.I. Tarr, M.A. Neill, J.H. Lewis, N. Hargrett-Bean, and J.M. Kobayashi. 1989. Toxin genotypes and plasmid profiles as determinants of systemic sequelae in *Escherichia coli* 0157:H7 infections. *J. Infect. Dis.* 160: 994–998.

38. Bitzan, M., K. Ludwig, M. Klemt, H. Koenig, J. Büren, and D.E. Müller-Wiefel. 1993. The role of *Escherichia coli* O157 infections in the classical (enteropathic) haemolytic uraemic syndrome: results of a Central European, multicentre study. *Epidemiol. Infect.* 110:183–196.

39. Biragyn, A., and S.A. Nedospasov. 1995. Lipopolysaccharide-induced expression of TNF-α gene in the macrophage cell line ANA-1 is regulated at the level of transcription processivity. *J. Immunol.* 155:674–683.

40. Sandvig, K., and B. van Deurs. 1994. Endocytosis and intracellular sorting of ricin and Shiga toxin. *FEBS Lett.* 346:99–102.

41. Shultz, P.J., and L. Raij. 1992. Endogenously synthesized nitric oxide prevents endotoxin-induced glomerular thrombosis. *J. Clin. Invest.* 90:1718–1725.

42. Kohan, D.E. 1997. Endothelins in the normal and diseased kidney. *Am. J. Kidney Dis.* 29:2–26.

43. Siegler, R.L. 1995. The hemolytic uremic syndrome. *Pediatr. Clin. N. Am.* 42:1505–1529.

44. Sawaf, H., M.J. Sharp, K.J. Youn, P.A. Jewell, and A. Rabbani. 1978. Ischemic colitis and stricture after hemolytic-uremic syndrome. *Pediatrics.* 61: 315–316.

45. Crisp, D.E., R.L. Siegler, J.F. Bale, and J.A. Thompson. 1981. Hemorrhagic cerebral infarction in the hemolytic-uremic syndrome. *J. Pediatr.* 99:273–276.

46. Siegler, R.L. 1994. Spectrum of extrarenal involvement in postdiarrheal hemolytic-uremic syndrome. *J. Pediatr.* 125:511–518.

47. Siegler, R.L., S.S. Edwin, R.D. Christofferson, and M.D. Mitchell. 1991. Endothelin in the urine of children with the hemolytic uremic syndrome. *Pediatrics.* 88:1063–1066.

48. Iwasaki, S., T. Homma, Y. Matsuda, and V. Kon. 1995. Endothelin receptor subtype B mediates autoinduction of endothelin-1 in rat mesangial cells. *J. Biol. Chem.* 270:6997–7003.

49. Gomez-Garre, D., R. Largo, X.H. Liu, S. Gutierrez, M.J. Lopez-Armada, I. Palacios, and J. Egido. 1996. An orally active ET_A/ET_B receptor antagonist ameliorates proteinuria and glomerular lesions in rats with proliferative nephritis. *Kidney Int.* 50:962–972.

50. Brooks, D.P. 1996. Role of endothelin in renal function and dysfunction. *Clin. Exp. Pharmacol. Physiol.* 23:345–348.

51. Reid, J.L., D. Dawson, and I.M. Macrae. 1995. Endothelin, cerebral ischaemia and infarction. *Clin. Exp. Hypertens.* 17:399–407.

52. Hof, R., A. Hof, and Y. Takiguchi. 1989. Massive regional differences in the vascular effects of endothelin. *J. Hypertens. Suppl.* 7:S274–S275.

53. Kurose, I., S. Miura, D. Fukumura, H. Tashiro, H. Imaeda, H. Shiozaki, M. Suematsu, H. Nagata, E. Sekizuka, and M. Tsuchiya. 1992. Role of platelet activating factor on the fibrinolytic activation in the pathogenesis of gastric mucosal damage induced by endothelin-1. *Gut.* 33:868–871.

54. Kuhn, M., M. Fuchs, F. Beck, S. Martin, J. Jahne, J. Klempnauer, V. Kaever, G. Rechkemmer, and W. Forssmann. 1996. Endothelin-1 potently stimulates chloride secretion and inhibits Na(+)-glucose absorption in human intestine in vitro. *J. Physiol. (Lond.).* 499:391–402.

55. Inagaki, H., A. Bishop, C. Escrig, J. Wharton, T. Allen-Mersh, and J. Polak. 1991. Localization of endothelinlike immunoreactivity and endothelin binding sites in human colon. *Gastroenterology.* 101:47–54.

56. Halim, A., N. Kanayama, E. el Maradny, K. Maehara, H. Masahiko, and T. Terao. 1994. Endothelin-1 increased immunoreactive von Willebrand factor in endothelial cells and induced micro thrombosis in rats. *Thromb. Res.* 76:71–76.

57. Kawana, M., M.E. Lee, E.E. Quertermous, and T. Quertermous. 1995. Cooperative interaction of GATA-2 and AP1 regulates transcription of the endothelin-1 gene. *Mol. Cell. Biol.* 15:4225–4231.

58. Zubiaga, A.M., J.G. Belasco, and M.E. Greenberg. 1995. The nonamer UUAUUUAUU is the key AU-rich sequence motif that mediates mRNA degradation. *Mol. Cell. Biol.* 15:2219–2230.

59. Lagnado, C.A., C.Y. Brown, and G.J. Goodall. 1994. AUUUA is not sufficient to promote poly(A) shortening and degradation of an mRNA: the functional sequence within AU-rich elements may be UUAUUUA(U/A)(U/A). *Mol. Cell. Biol.* 14:7984–7995.

60. Gerez, L., G. Arad, S. Efrat, M. Ketinel, and R. Kaempfer. 1995. Post-transcriptional regulation of human interleukin-2 gene expression at processing of precursor transcripts. *J. Biol. Chem.* 270:19569–19575.

61. Ross, J. 1995. mRNA stability in mammalian cells. *Microbiol. Rev.* 59: 423–450.

62. Jacobson, A., and S.W. Peltz. 1996. Interrelationship of the pathways of mRNA decay and translation in eukaryotic cells. *Annu. Rev. Biochem.* 65:693–739.

63. Tesh, V.L., B. Ramegowda, and J.E. Samuel. 1994. Purified Shiga-like toxins induce expression of proinflammatory cytokines from murine peritoneal macrophages. *Infect. Immun.* 62:5085–5094.

64. Ramegowda, B., and V.L. Tesh. 1996. Differentiation-associated toxin receptor modulation, cytokine production, and sensitivity to Shiga-like toxins in human monocytes and monocytic cell lines. *Infect. Immun.* 64:1173–1180.

65. van Setten, P.A., L.A.H. Monnens, R.G.G. Verstraten, L.P.W.J. van den Heuvel, and V.W.M. van Hinsbergh. 1996. Effects of verocytotoxin-1 on nonadherent human monocytes: binding characteristics, protein synthesis, and induction of cytokine release. *Blood.* 88:174–183.

66. Harel, Y., M. Silva, B. Giroir, A. Weinberg, T.B. Cleary, and B. Beutler. 1993. A reporter transgene indicates renal-specific induction of tumor necrosis factor (TNF) by shiga-like toxin. Possible involvement of TNF in hemolytic uremic syndrome. *J. Clin. Invest.* 92:2110–2116.

67. Knight, B. 1979. Ricin—a potent homicidal poison. *Br. Med. J.* 278:350–351.

68. Farkas-Himsley, H., R. Hill, B. Rosen, S. Arab, and C.A. Lingwood. 1995. The bacterial colicin active against tumor cells in vitro and in vivo is verotoxin 1. *Proc. Natl. Acad. Sci. USA.* 92:6996–7000.

69. Simpson, J.C., C. Dascher, L.M. Roberts, J.M. Lord, and W.E. Balch. 1995. Ricin cytotoxicity is sensitive to recycling between the endoplasmic reticulum and the Golgi complex. *J. Biol. Chem.* 270:20078–20083.

70. Vater, C.A., L.M. Bartle, J.D. Leszyk, J.M. Lambert, and V.S. Goldmacher. 1995. Ricin A chain can be chemically cross-linked to the mammalian ribosomal proteins L9 and L10e. *J. Biol. Chem.* 270:12933–12940.

71. Iordanov, M.S., D. Pribnow, J.L. Magun, T.H. Dinh, J.A. Pearson, S.L.Y. Chen, and B.E. Magun. 1997. Ribotoxic stress response: activation of the stress-activated protein kinase JNK1 by inhibitors of the peptidyl transferase reaction and by sequence-specific RNA damage to the α-sarcin/ricin loop in the 28S rRNA. *Mol. Cell. Biol.* 17:3373–3381.